Monthly Notices of the ROYAL ASTRONOMICAL SOCIETY

MNRAS **492,** 1543–1549 (2020) doi:10.1093/mnras/stz3192
Advance Access publication 2019 November 19

Satellites of satellites: the case for Carina and Fornax

Stephen A. Pardy,[1] Elena D'Onghia,[1,2★] Julio F. Navarro,[3★†] Robert Grand,[4] Facundo A. Gómez,[5,6] Federico Marinacci,[7] Rüdiger Pakmor,[4] Christine Simpson[8,9] and Volker Springel[4]

[1]*Department of Astronomy, University of Wisconsin, 475 North Charter Street, Madison, WI 53706, USA*
[2]*Center for Computational Astrophysics, Flatiron Institute, 162 Fifth Avenue, New York, NY 10010, USA*
[3]*Department of Physics and Astronomy, University of Victoria, Victoria, BC V8P 5C2, Canada*
[4]*Max-Planck-Institut für Astrophysik, Karl-Schwarzschild-Str. 1, D-85748 Garching, Germany*
[5]*Instituto de Investigación Multidisciplinar en Ciencia y Tecnología, Universidad de La Serena, Raúl Bitrán 1305, La Serena, Chile*
[6]*Departamento de Física y Astronomía, Universidad de La Serena, Av. Juan Cisternas 1200 Norte, La Serena, Chile*
[7]*Department of Physics and Astronomy, University of Bologna, via Gobetti 93/2, I-40129 Bologna, Italy*
[8]*Enrico Fermi Institute, The University of Chicago, Chicago, IL 60637, USA*
[9]*Department of Astronomy and Astrophysics, The University of Chicago, Chicago, IL 60637, USA*

Accepted 2019 November 5. Received 2019 October 19; in original form 2019 March 20

ABSTRACT

We use the Auriga cosmological simulations of Milky Way (MW)-mass galaxies and their surroundings to study the satellite populations of dwarf galaxies in lambda-cold dark matter. As expected from prior work, the number of satellites above a fixed stellar mass is a strong function of the mass of the primary dwarf. For galaxies as luminous as the Large Magellanic Cloud (LMC), and for haloes as massive as expected for the LMC (from its rotation speed), the simulations predict about ∼3 satellites with stellar masses exceeding $M_* > 10^5\,\mathrm{M}_\odot$. If the LMC is on its first pericentric passage, then these satellites should be near the LMC and should have orbital angular momenta roughly coincident with that of the LMC. We use 3D positions and velocities from the 2nd data release of the *Gaia* mission to revisit which of the 'classical' MW dwarf spheroidals could plausibly be LMC satellites. The new proper motions of the Fornax and Carina dwarf spheroidals place them on orbits closely aligned with the orbital plane of the Magellanic Clouds, hinting at a potential Magellanic association. Together with the Small Magellanic Cloud (SMC), this result raises to 3, the number of LMC satellites with $M_* > 10^5\,\mathrm{M}_\odot$, as expected from simulations. This also fills the 12 mag luminosity gap between the SMC and the ultrafaints Hyi1, Car2, Hor1, and Car3, the few ultrafaint satellites confirmed to have orbits consistent with a Magellanic origin.

Key words: galaxies: dwarf – Local Group.

1 INTRODUCTION

In the current paradigm of structure formation, the lambda-cold dark matter (ΛCDM) scenario, the mass function of substructures in a dark matter halo ('subhaloes') is approximately self-similar. This means that, expressed in units of the primary halo mass, the mass function of subhaloes is independent of the primary, and well approximated by a steep power law (Moore et al. 1999; Springel et al. 2008; Boylan-Kolchin et al. 2009; Wang et al. 2012).

The similarity is broken when considering the stellar mass function of satellite galaxies in clusters, groups, and around individual primaries. Clusters have far more 'substructure' (i.e. more satellite galaxies of a given scaled mass) than groups, and groups have more satellites than isolated bright primaries. The difference arises because the relation between galaxy stellar mass (M_*) and halo virial[1] mass, M_{200}, is highly non-linear, thus breaking the similarity.

Indeed, had M_* and M_{200} been related by a simple power law, then the scaled satellite luminosity function, $N(>\mu)$ (where $\mu = M_*^{\rm sat}/M_*^{\rm pri}$) would be independent of the primary mass. This independence is actually expected in the dwarf galaxy regime, where

★ E-mail: edonghia@astro.wisc.edu (ED); jfn@uvic.ca (JFN)
† CIfAR Fellow.

[1]We define the virial mass of a halo, M_{200}, as that enclosed within a radius, r_{200}, where the mean inner density is 200 times the critical density for closure. We refer to virial quantities as those measured at or within that radius, and denote them with a '200' subscript.

ΛCDM galaxy formation models [based on abundance-matching (AM) techniques and simulations] predict a steep, near power-law dependence of M_* on M_{200} over a wide range of stellar masses above and below $\sim 10^8$ $M_\odot$. In other words, the scaled satellite luminosity function of dwarf primaries should be nearly independent of the stellar mass of the primary at least over some range of primary mass (Sales et al. 2012). This independence is expected to break down for small primary masses, however, as satellites start probing the minimum halo mass 'threshold' needed to form a luminous system imposed by cosmic reionization and stellar feedback (see e.g. Ferrero et al. 2012; Fattahi et al. 2018).

In particular, these models predict roughly ∼4–5 satellites within 10 mag of the primary for dwarfs as luminous as the Large and Small Magellanic Clouds (hereafter LMC and SMC, respectively). Because of its insensitivity to the actual primary mass, this is a robust prediction that may be tested by searching for dwarf galaxies that might have plausibly been associated with the Clouds at the time of their infall into the Milky Way (MW) halo.

The search for Magellanic satellites, in fact, has a long history, tracing back to the proposal by Lynden-Bell (1976) of a 'Greater Magellanic Galaxy' system of dwarfs in the MW halo (Lynden-Bell 1982). D'Onghia & Lake (2008) emphasized that groups of dwarfs were a natural prediction of hierarchical models of galaxy formation, and went further to suggest that the LMC and SMC were the largest members of a group of dwarf galaxies that has been recently accreted into the MW and that could include up to 7 of the 11 brightest MW satellites.

The dwarf group accretion idea was further elaborated using *N*-body simulations by a number of authors (Li & Helmi 2008; Lux, Read & Lake 2010; Nichols et al. 2011; Deason et al. 2015; Jethwa, Erkal & Belokurov 2016), and has often been cited as a possible explanation for the dynamical peculiarities of the MW satellite population (see e.g. Pawlowski 2018, for a recent review).

A major step towards identifying true Magellanic satellites came from new estimates of the proper motion of the LMC, made possible by painstaking astrometric measurements of *Hubble Space Telescope* images over different epochs (Kallivayalil et al. 2006). These measurements showed that the tangential velocity of the LMC is much larger than its radial velocity, and also much larger than the expected circular velocity at its present distance of ∼50 kpc from the Galactic centre (see e.g. D'Onghia & Fox 2016, for a recent review). This implies long orbital periods and, in most currently favoured models, that the LMC is near its first pericentric approach to the Galaxy (see e.g. Besla et al. 2007).

If the LMC is on its first approach, then most Magellanic satellites should lie close to the LMC because the Galactic tidal field has not yet had enough time to disperse them (Sales et al. 2011). Indeed, these authors identified the surroundings of the LMC as 'fertile hunting ground for faint, previously unnoticed MW satellites', including Magellanic satellites as well. This prediction came spectacularly true with the recent discoveries of over 30 candidate dwarf galaxies in close sky proximity to the Clouds, thanks to surveys like the Dark Energy Survey, the Magellanic Satellites Survey, SMASH, and Pan-STARRS (Bechtol et al. 2015; Drlica-Wagner et al. 2015; Kim & Jerjen 2015; Kim et al. 2015; Koposov et al. 2015; Laevens et al. 2015; Martin et al. 2015; Drlica-Wagner et al. 2016; Luque et al. 2016; Koposov et al. 2018; Torrealba et al. 2018).

The first-approach scenario further restricts the range of distances, velocities, and sky positions of previously associated Magellanic satellites, as they should lead or trail the Clouds on orbits consistent with their tidal debris. Using these criteria, Sales et al. (2011) found little evidence for a clear association between any of the 'classical' (i.e. $M_V < -8$) dwarf spheroidals and the LMC: only the SMC emerged from that analysis as a clear companion of the LMC.

These authors further argued that the most stringent test of association with the Clouds is provided by the orbital angular momentum of a satellite around the MW, whose direction must be roughly coincident with the Clouds. Using proper motion data available at the time, they ruled out Fornax and Carina as Magellanic satellites, despite some favourable indications from their distances and radial velocities. Sales et al. (2017) and Kallivayalil et al. (2018) extended this method to the 'ultrafaint' (i.e. $M_V > -8$) satellite population, and their combined work was able to show that at least *4* such satellites (Hor1, Car2, Car3, and Hyi1) are very likely associated with the Clouds.

Although this finding provides strong support for the hierarchical clustering of dwarfs, it also raises an interesting question about the luminosity function of the Magellanic association. The LMC has a fairly massive companion, the SMC, which is about 1.5 mag fainter than the LMC, but its next most luminous satellite appears to be Hyi1, which is nearly 13 mag fainter. This leaves a >10 mag 'gap' in the satellite luminosity function that seems peculiar given the number of massive substructures expected for a halo containing a galaxy as luminous as the LMC (Springel et al. 2008).

We revisit these issues here using cosmological hydrodynamical simulations of the formation of MW-mass galaxies and their surroundings from the Auriga Project (Grand et al. 2017). Our main aims are to explore the predictions of these models for the abundance of luminous satellites around galaxies like the LMC and to re-examine the association of some of the classical MW dSphs with the Clouds using the latest proper motions andThe blue circles have radii of 10°, 20°, and 30° from the direction of the LMC's angular momentum orbital parameters of MW satellites from '*Gaia* DR2', the second data release of the *Gaia* mission (Fritz et al. 2018; Kallivayalil et al. 2018; Simon 2018; Helmi, van Leeuwen & McMillan 2018).

This paper is organized as follows. In Section 2, we discuss the Auriga simulations (Section 2.1), and how the simulated galaxy sample was selected and analysed (Section 2.2). Our results are described in Section 3, and a comparison with *Gaia* DR2 is presented in Section 3.2. A summary of our main findings is given in Section 4.

2 METHODS

2.1 The Auriga simulations

We use 40 ΛCDM cosmological high-resolution magneto-hydrodynamic zoomed-in simulations of the formation of MW analogues from the Auriga project (Grand et al. 2017). The MW analogues have haloes with virial masses in the range between 5×10^{11} and 2×10^{12} $M_\odot$. The haloes were identified at redshift $z = 0$ as isolated systems in a dark matter-only simulation of a 100^3 Mpc^3 volume from the EAGLE project (Schaye et al. 2015). The isolation criteria imply that each halo selected for resimulation is at least as far as nine virial radii from any other halo with mass greater than 3 per cent of the selected halo mass.

The initial conditions for the zoom resimulations of the target haloes were created at $z = 127$, and adopt the following cosmological parameters: $\Omega_m = 0.307$, $\Omega_b = 0.048$, $\Omega_\Lambda = 0.693$, and a Hubble constant of $H_0 = 100\,h$ km s^{-1} Mpc^{-1}, where $h = 0.6777$.

The selected haloes are then resimulated at higher resolution with full baryonic physics.

The simulations were performed with the moving mesh code AREPO (Springel 2010), including magnetohydrodynamics (Pakmor et al. 2016) and a comprehensive galaxy formation model (see Springel & Hernquist ; Vogelsberger et al. 2013; Marinacci, Pakmor & Springel 2014 and especially Grand et al. 2017, for more details). The model includes: primordial and metal line cooling; a prescription for a uniform background UV field that completes reionization at $z = 6$ (Faucher-Giguere et al. 2009); a subgrid model for a multi-phase interstellar medium (ISM), star formation, and stellar feedback; black hole seeding, accretion, and feedback; and magnetic fields. Note that the presence of magnetohydrodynamics is expected to have little effect on the global properties of the MW stellar disc and almost no effect on the properties of satellites of the MW (see e.g. Marinacci & Vogelsberger 2016; Pakmor et al. 2017).

We briefly describe the physical processes included in the Auriga simulations. The ISM is described by a subgrid model first presented in Springel & Hernquist (2003), in which star-forming gas is treated as a two-phase medium: a phase of cold, dense clouds embedded in a hot medium. The gas is set to be thermally unstable for densities higher than a threshold density, which is assumed to be $n = 0.13\,\mathrm{cm}^{-3}$. The motivation for the ISM model comes from the assumption that the small scale processes that describe the mass fractions of molecular clouds and ambient gas, such as radiative cooling, thermal conduction, star formation and feedback, quickly establish a pressure equilibrium between the hot and cold phases. In this regime, the gas pressure is a function of density only.

SNII feedback is modelled by an isotropic, non-local mass and momentum injection that yields a kinetic wind emanating from the surface of star-forming regions. Technically, this is implemented by creating 'wind particles' that travel from their launch sites until the density drops below the star formation threshold. At this point, their momentum and mass are added to the corresponding local gas cells. Primordial and metal-line cooling with self-shielding corrections is enabled. A spatially uniform UV background field is included, which completes reionization at redshift $z = 6$. Feedback from black holes is implemented in two phases: a radio mode for low accretion rates and a quasar mode for high accretion rates [see Grand et al. (2017) for details of the subgrid physics].

In this paper, we focus on the medium-resolution simulations of the Auriga suite, which correspond to the 'level 4' resolution described in Grand et al. (2017). This is because the number of high-resolution Auriga runs is limited, combined with the fact that not every run has an extra isolated halo massive enough to host an LMC-like galaxy. Note that a convergence study of the satellite luminosity function of the main hosts between the 'level 3' and 'level 4' simulations is provided in the appendix of Grand et al. (2017).

The typical dark-matter particle mass is $\sim 3 \times 10^5\,\mathrm{M}_\odot$, and the baryonic mass resolution is $\sim 5 \times 10^4\,\mathrm{M}_\odot$. The physical softening of collisionless particles is fixed in comoving coordinates and increases in physical units up to a maximum length of 369 pc, which is reached at $z = 1$. The physical-softening value for the gas cells is scaled by the gas-cell radius (assuming a spherical cell shape given the volume), with a minimum gravitational softening set to that of the collisionless particles.

Each high-resolution volume is embedded in a larger region containing progressively higher mass boundary particles. The uncontaminated high-resolution region typically extends beyond $3 \times r_{200}$, but is highly non-spherical.

2.2 Simulated galaxy sample selection

Structures in the Auriga volumes are identified using a two-step process. First, the standard 'friends-of-friends (FOF)' algorithm (Davis et al. 1985) groups particles together using a fixed linking length, chosen to be 0.2 of the mean interparticle separation. Then, the 'subfind' algorithm (Springel et al. 2001) recursively identifies gravitationally bound groups, identifying the subhaloes within each FOF halo.

For this work, we select all unique FOF groups that are uncontaminated by boundary particles at the present day (they must be more than 750 kpc from the nearest boundary particle). The central galaxy of each FOF group is designated as the 'primary' or 'host' galaxy of its group. We measure the stellar mass and other quantities of interest of central host galaxies using only particles within $r_{\mathrm{gal}} = 0.15\,r_{200}$. Subhaloes within two virial radii of each central are labelled as its 'satellites'. This choice is made in order to include most subhaloes that have, at some point in the past, been within the virial radius of the host (Ludlow et al. 2009). We have verified that none of our conclusions are drastically affected if 'satellites' are defined as those within one virial radius, rather than two. Note that many low-mass subhaloes contain no stars, i.e. they are 'dark'.

3 RESULTS

Fig. 1 shows the stellar mass versus halo virial mass (SMHM) relation for all primary galaxies in our sample, selected at $z = 0$. This figure also shows the dependence of the stellar mass on the maximum circular velocity of each system, V_{max}, an alternative measure of halo mass that is more appropriate for satellites, for which a virial mass cannot be defined.

For reference, we show the AM relation of Behroozi et al. (2013) in the left-hand panel of Fig. 1. Auriga galaxies seem to have, on an average, more stars than indicated by the AM relation, a result discussed in detail by Grand et al. (2017) and Simpson et al. (2017). We also include the M_*–V_{max} relation reported by Fattahi et al. (2018) for the APOSTLE suite of Local Group cosmological simulations run with the EAGLE code. These have been shown to match fairly well the mass function and internal structure of Local Group dwarfs (Sawala et al. 2016).

Auriga again seems to predict slightly more massive galaxies than APOSTLE over the whole halo mass range. For the purposes of this analysis, this may be taken to suggest that our predictions for the satellite luminosity function of dwarfs should be treated as upper limits.

Note as well that both the SMHM and M_*–V_{Max} relation are rather tight. This implies that for given stellar mass, the halo mass of a primary galaxy is well constrained. The reverse is not true, especially at low masses, where the steepness of the relation precludes an accurate prediction of the stellar mass of a galaxy at given halo mass.

3.1 Satellites of dwarfs

We explore next the satellite population of the primary galaxies shown in Fig. 1. Although the subhalo mass function is expected to be self-similar, as discussed in Section 1, the luminous satellite population is expected to depend strongly on halo mass and, consequently, on the stellar mass of the host galaxy. We show this in Fig. 2, where we have grouped the centrals in bins of halo mass (left-hand panel) and of central stellar mass (right-hand panel).

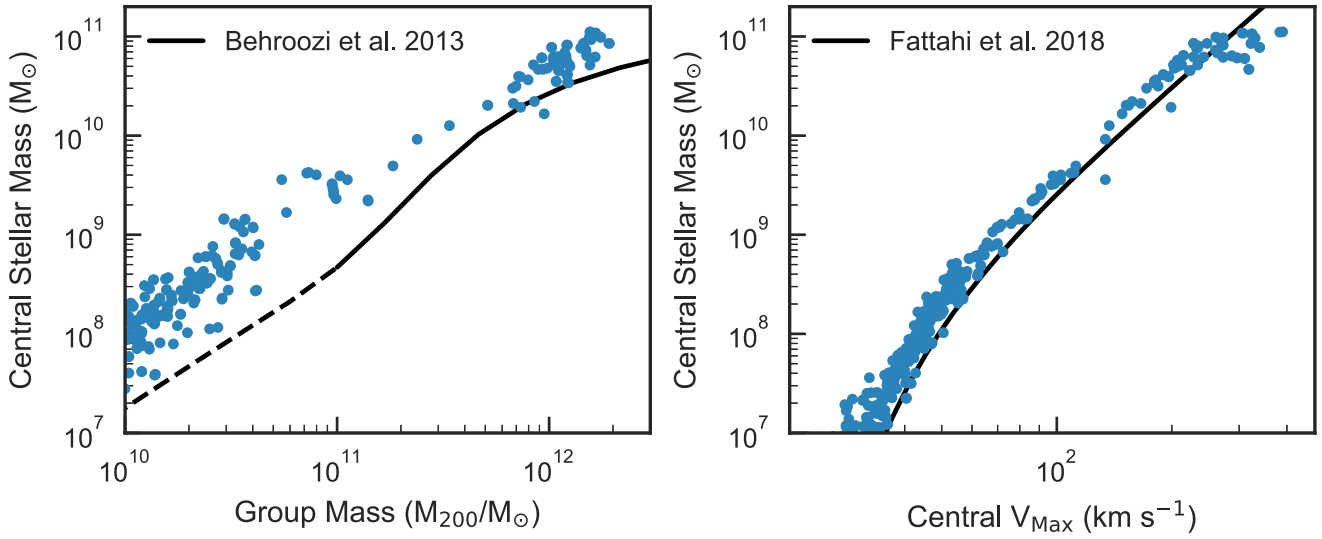

Figure 1. Left: Stellar mass versus virial mass for central galaxies in our Auriga sample (blue points), compared with the AM relation from Behroozi, Wechsler & Conroy (2013) (black line). The dashed region of the Behroozi et al. (2013) relation below 10^{11} M$_\odot$ is the extrapolation of their stellar mass–halo mass relation to lower masses. Right: Galaxy stellar mass versus maximum circular velocity, $V_{\rm max}$, an alternative measure of halo mass, for central galaxies in our sample (blue points), compared with the equivalent relationship for the APOSTLE simulations reported by Fattahi et al. (2018). The central galaxy stellar mass is measured within $r_{\rm gal} = 0.15\, r_{200}$.

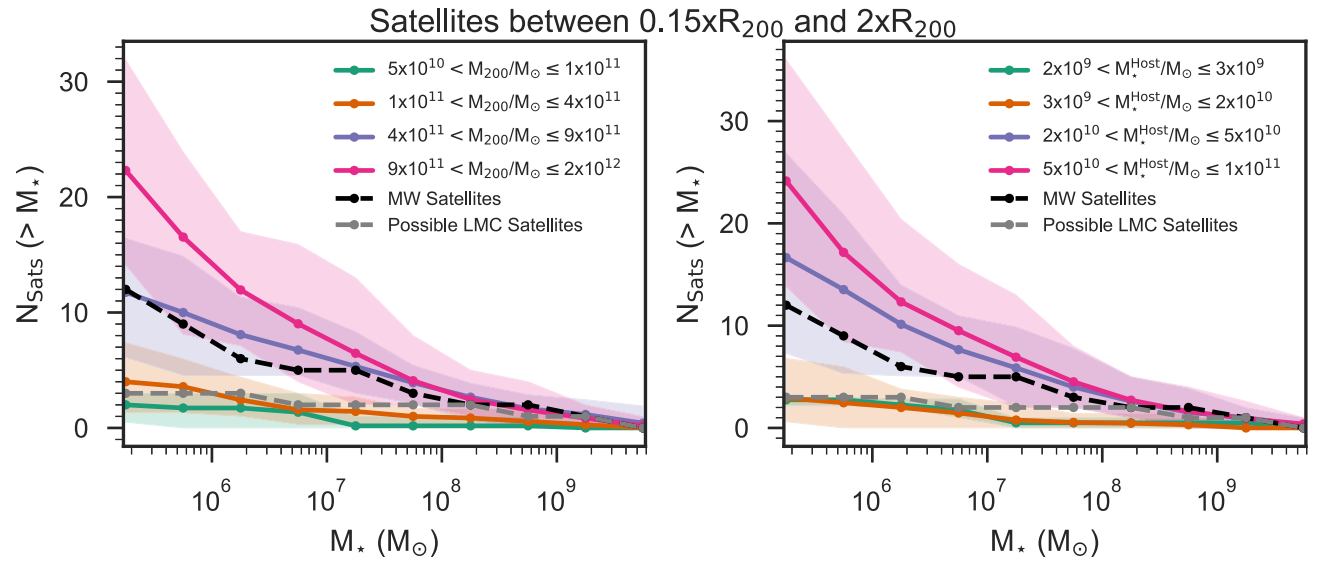

Figure 2. The cumulative number of satellites above a given stellar mass. We measure this quantity for FOF groups selected by mass, and show the median (solid line with points) and inner 90 per cent of the distribution (shaded region) for the cumulative abundance function of all FOF groups in each selection. We also include the observed cumulative satellite stellar mass function for the MW from McConnachie (2012), which we show in the black dashed line. We also show the possible LMC satellites: SMC, Fornax, and Carina (in order of decreasing mass) as a grey dashed line. Left: FOF groups selected by M_{200}. Right: FOF groups selected by central galaxy $M_\star$.

The number of 'luminous' satellites, defined as those with $M_\star > 10^5$ M$_\odot$ (roughly the stellar mass of the Draco dwarf spheroidal, the faintest of the 'classical' dSphs, with $M_{\rm V} \sim -8$), is a strong function of the mass of the system. For an LMC-like primary, with a stellar mass of 2×10^9 M$_\odot$, these results indicate that we should expect of the order of ∼3 satellites at least as bright as Draco.[2]

[2]We caution the reader that satellites with $M_\star \sim 10^5$ M$_\odot$ contain relatively few stellar particles, so that mass discretization may add some uncertainty to our results.

However, we have only 6 primaries in our sample in the range $2 \times 10^9 < M_\star/{\rm M}_\odot < 3 \times 10^9$, and therefore the uncertainties on this average are difficult to estimate. Over the wider primary mass range of $2 \times 10^9 < M_\star/{\rm M}_\odot < 2 \times 10^{10}$ (where our sample has 18 primaries), the median number of satellites is 3 and the 90th percentiles span the range 1–7.

One could also use the halo mass to estimate the expected number of satellites, but this requires assuming a total halo mass for the LMC. AM models, for example, suggest a virial mass for the LMC of at least 1.6×10^{11} M$_\odot$ (Moster et al. 2010; Guo et al. 2011), or

as high as $\sim 2 \times 10^{11}\,\mathrm{M}_\odot$ (Behroozi et al. 2013). Alternatively, assuming that the rotation speed of the LMC [about $70\,\mathrm{km\,s^{-1}}$ according to Alves & Nelson (2000)] matches the virial velocity of its halo indicates a total mass of the order of $\sim 1.1 \times 10^{11}\,\mathrm{M}_\odot$. The study of van der Marel & Kallivayalil (2014) reports a higher circular velocity of $\sim$90 $\mathrm{km\,s^{-1}}$ within $\sim$9 kpc, implying an even higher virial mass of the order of $\sim 2.4 \times 10^{11}\,\mathrm{M}_\odot$. Finally, the presence of a satellite as massive as the SMC ($M_\star > 10^9\,\mathrm{M}_\odot$) further supports a heavy LMC, at least in our Auriga runs. Indeed, we find no satellites as massive as the SMC around hosts with $M_{200} < 10^{11}\,\mathrm{M}_\odot$.

In any case, for any of the LMC halo masses quoted above, the predicted number of luminous satellites is still expected to be of the order of $\sim$3 or more (see the left-hand panel of Fig. 2). This is actually consistent with the recent study of Dooley et al. (2017), who applied AM techniques to the dark matter-only simulations of the `Caterpillar` project and report 1–6 satellites with $M_\star > 10^5\,\mathrm{M}_\odot$ within the virial volume of isolated LMC-sized galaxies.

The agreement between our simulations and the AM-based analysis of Dooley et al. (2017) is, at face value, surprising, given the systematic offset between AM and the stellar mass of Auriga centrals (left-hand panel of Fig. 1). In particular, one might have expected a much larger number of luminous satellites in Auriga, given the larger simulated stellar masses at given halo mass.

This, however, is not the case, mainly because many low-mass haloes in the simulations are 'dark' (e.g. Sawala et al.), an issue that is difficult to implement in AM models and that makes their application uncertain. The corrections are not small; indeed, the fraction of 'dark' subhaloes (i.e. systems that fail to form a single star particle in the Auriga level 4 runs) climbs from 0 to more than 90 per cent in the narrow mass range between $V_{\rm max} = 30$ and $10\,\mathrm{km\,s^{-1}}$. Accounting for this 'dark fraction' is critical for predicting the number of satellites as faint as $M_\star > 10^5\,\mathrm{M}_\odot$. As a result, models with rather different SMHM may yield the same number of faint satellites if they assume different dark fractions, as seems to be the case when comparing the results of Dooley et al. (2017) with ours. A detailed comparison with their modelling is beyond the scope of our analysis but, for the purposes of our discussion, we regard it as reassuring that, despite the large modelling differences, the predicted number of $M_\star > 10^5\,\mathrm{M}_\odot$ satellites of LMC-sized hosts seem to be fairly robust.

Finally, we note that the LMC has one known satellite, the SMC, but the next brightest confirmed satellite, Hyi1, has $M_{\rm V} \sim -4.7$, or a stellar mass of the order of $\sim 5 \times 10^3\,\mathrm{M}_\odot$ (Kallivayalil et al. 2018), suggestive of a large 'gap' in the LMC satellite luminosity function. Does this suggest that the halo mass of the LMC is substantially smaller than suggested by either AM or its rotation speed? Or that somehow some of the classical dSphs have a yet-unrecognized Magellanic origin, as suggested by Lynden-Bell (1976) and D'Onghia & Lake (2008)?

3.2 The Magellanic association of classical dSphs

The possible association of the classical MW dSphs with the Clouds was studied in detail by Sales et al. (2011), who concluded that there was no strong evidence for any of them to have a Magellanic origin. However, these authors also cautioned that their conclusion should be revisited when better proper motion data became available. Their criteria for Magellanic association hinges on a few simple indicators: (i) sky proximity to the Clouds, (ii) position, distance, and radial velocity consistent with tidal debris from the Clouds, and (iii) orbital angular momentum direction coincident with the Clouds.

Criterion (i) is motivated by the fact that, if the Clouds are on their first pericentric passage about the MW then the tidal field has not yet had time to fully disperse the Magellanic group. Most such satellites, like the Clouds, are thus expected to be near the pericentre of their orbits around the MW.

Criterion (ii) applies to satellites that lag behind or have sped ahead of the Clouds, following approximately the orbital plane traced by the Magellanic orbit. If behind the Clouds, the satellite must still be infalling, and therefore should have negative Galactocentric radial velocity, while if ahead of the Clouds, the satellite must be past pericentre, and should therefore have positive radial velocities.

Finally, criterion (iii) can only be applied to systems with accurate 3D velocity and position estimates, but is perhaps the most telling. This is because the Magellanic system is much less massive than the MW and its orbital velocity today is much higher than the likely velocity dispersion of its satellite system. Therefore, all of its associated satellites must approximately share the same orbital plane, which implies that the direction of their orbital angular momenta must be very similar to that of the LMC.

Following these criteria, the Sagittarius dSph is easily excluded because its orbital plane is nearly perpendicular to that of the LMC (i.e. the Magellanic Stream is nearly perpendicular to the Sagittarius stream, although they both roughly trace polar orbits). Draco and Ursa Minor are so far away from the Clouds (almost diametrically opposite on the sky) that it is hard to make a case for association. Sextans and Sculptor have radial velocities inconsistent with their position on the sky if they had been stripped from the LMC. Tucana and Hercules are also easily excluded given their distances, positions, and velocities. We refer the interested reader to Sales et al. (2011) for details.

On the other hand, the SMC passes all of these criteria for association. Fornax and Carina are more problematic. Although they pass criteria (i) and (ii), the proper motions available at the time of Sales et al. (2011) indicated that their orbits were not aligned with that of the Clouds. It is important to review the possible association of these systems now that more precise proper motions are available from the *Gaia* DR2.

Using velocities reported by Helmi et al. (2018), and auxiliary data from McConnachie (2012), Sales et al. (2017), Fritz et al. (2018), and Simon (2018), we compute the orbital angular momentum of all 10 'classical' MW dSphs and many of the ultrafaint dwarf galaxies. We show the direction of the angular momentum vector projected on to Galactic coordinates in Fig. 3. We indicate in red the 3 satellites that were selected based on the location and radial velocity criteria above. The contours indicate loci of fixed α, where α is the angle between $\vec{L}_{\rm LMC}$ and $\vec{L}_{\rm sat}$. The new measurements indicate that Fornax and Carina, which Sales et al. (2011) had concluded were unlikely Magellanic companions, are now clear candidates for Magellanic association.

The addition of Fornax and Carina would bring to 3, the total number of dwarfs more massive than $10^5\,\mathrm{M}_\odot$ associated with the LMC, and would also fill the 'luminosity gap' in the Magellanic satellite luminosity function between the SMC and Hyi1, bringing it into excellent agreement with the results of the simulations discussed above.

Before these conclusions can be fully accepted, however, a number of issues need to be resolved. One is that, at least when using the MW mass model adopted by Helmi et al. (2018), the eccentricity of Fornax's orbit is quite different from that of the LMC. Whereas

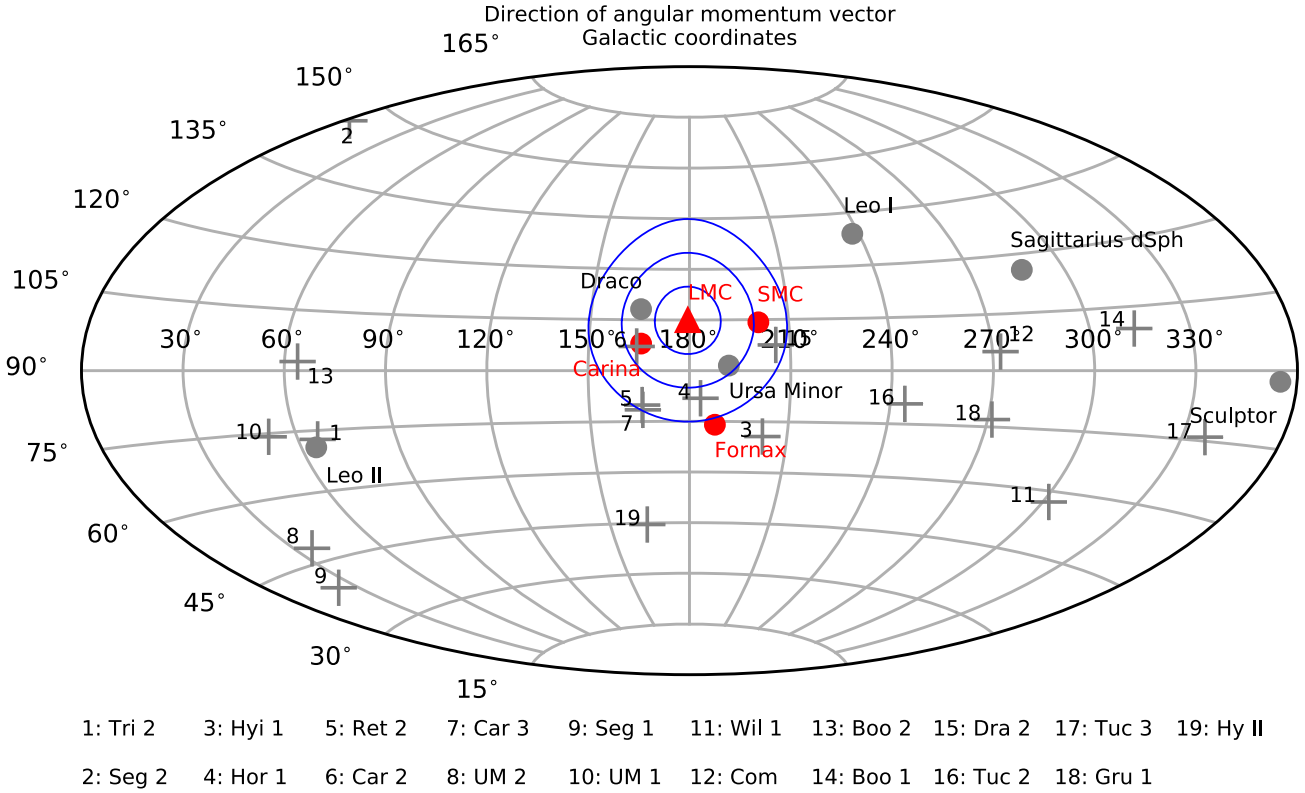

Figure 3. The direction of the orbital angular momentum vectors in Galactocentric coordinates for MW dwarf galaxies, using data from McConnachie (2012), Sales et al. (2017), Fritz et al. (2018), Helmi et al. (2018), and Simon (2018). Luminous dwarf galaxies (i.e. $M_V < -8$) are shown as circles, while ultrafaint galaxies are shown as crosses. Luminous dwarfs that are possible candidates of the LMC are shown in red, and others are shown in grey. The blue circles have radii of 10°, 20°, and 30° from the direction of the LMC's angular momentum.

the LMC is on a highly radially biased orbit, Fornax appears to follow a much less eccentric orbit. Another is that although Fornax is close in the sky to the Clouds, it is actually much farther away, at a distance of ∼130 kpc, compared to ∼50 kpc for the LMC.

Addressing these issues satisfactorily requires more sophisticated modelling, where the accretion of the Magellanic system in the evolving Galactic potential is taken into account. For example, Fornax orbits are usually computed assuming a static spherical halo potential, which is bound to be a poor approximation, especially in the Southern hemisphere and near the Clouds, whose own halo may disturb the orbit calculations and deflect the motions of other satellites (see e.g. Erkal et al. 2018). These questions are best addressed with direct numerical simulations, where a realistic population of Magellanic satellites (and its surroundings, which may be associated with filamentary accretion; Shao et al. 2018) should be evolved in a live, evolving MW + LMC potential. We plan to address these issues in future work.

4 CONCLUSIONS

We have studied the mass function of the satellites of dwarf galaxies using the Auriga project, a set of 40 high-resolution magnetohydrodynamical simulations of the formation of MW-like galaxies in the ΛCDM cosmogony. These simulations indicate that most isolated galaxies as massive as the LMC should be accompanied, on an average, by about ∼3 satellites at least as massive as $M_\star = 10^5\,\mathrm{M}_\odot$, or equivalently, at least as luminous as $M_V = -8$. This theoretical expectation is at odds with the results of earlier work, who argued that, aside from the SMC, the second brightest confirmed Magellanic satellite would be Hyi1, with an absolute magnitude of −4.7 (Sales et al. 2011, 2017; Kallivayalil et al. 2018). This implies an unexpected deficit of relatively luminous Magellanic satellites and a surprising gap of more than 10 mag in its satellite luminosity function.

This result may be explained in a number of ways. One is simply to accept that the Clouds have an odd assortment of satellites, with an overly massive one (the SMC) and a large gap to the ultrafaint regime. Another is that some bright satellites may have been missed because of their extreme low-surface brightness. The example of Crater II, a fairly massive ($M_* \sim 10^5\,\mathrm{M}_\odot$) MW satellite only discovered in 2016 because of its unusually low-surface brightness (Torrealba et al. 2016), gives credence to this possibility. Finally, there is the possibility that some of the classical MW dSphs are actually Magellanic satellites, as suggested by D'Onghia & Lake (2008).

We have revisited the possibility that the Fornax and Carina dSphs might be associated with the Clouds using new proper motions from *Gaia* DR2 and find that these make them strong candidates for being Magellanic satellites. Indeed, the new 3D velocities of these satellites put them on orbits with angular momentum directions closely aligned with that of the Clouds. The Draco and Ursa Minor dSphs also share this orbital plane, but their position in the northern sky, almost diametrically opposite to the Clouds, lessens the likelihood of association. The proximity of Fornax and

Carina to the Clouds in the southern sky bolsters the argument for association.

The addition of Fornax and Carina to the Magellanic trove of satellites would resolve the puzzling gap in its satellite luminosity function, bringing observations in close agreement with simulation expectations. Further work should focus on whether this association can be disproved using fully self-consistent, live direct numerical simulation of the evolution of Magellanic analogues, including its satellites, as they are accreted into the evolving Galactic potential.

ACKNOWLEDGEMENTS

EDO acknowledges support from the Vilas Associate Research Fellowship and thanks the Center for Computational Astrophysics for the hospitality during the completion of this work. JFN acknowledges the hospitality of the KITP at UC Santa Barbara and of the Aspen Center for Physics, where this research was partially carried out. FM acknowledges support through the Program 'Rita Levi Montalcini' of the italian MIUR. KITP is supported in part by the National Science Foundation under Grant No. NSF PHY-1748958. The ACP is supported by National Science Foundation grant PHY-1607611. This research made extensive use of many open-source Python packages including the Pathos (http://trac.mystic.cacr.caltech.edu/project/pathos) multiprocessing library (McKerns et al. 2012), and the Scipy ecosystem (Hunter 2007; Perez & Granger 2007; van der Walt, Colbert & Varoquaux 2011).

REFERENCES

Alves D. R., Nelson C. A., 2000, ApJ, 542, 789
Bechtol K. et al., 2015, ApJ, 807, 50
Behroozi P. S., Wechsler R. H., Conroy C., 2013, ApJ, 770, 57
Besla G., Kallivayalil N., Hernquist L., Robertson B., Cox T. J., van der Marel R. P., Alcock C., 2007, ApJ, 668, 949
Boylan-Kolchin M., Springel V., White S. D. M., Jenkins A., Lemson G., 2009, MNRAS, 398, 1150
D'Onghia E., Lake G., 2008, ApJ, 686, L61
D'Onghia E., Fox A. J., 2016, ARA&A, 54, 363
Davis M., Efstathiou G., Frenk C. S., White S. D. M., 1985, ApJ, 292, 371
Deason A. J., Wetzel A. R., Garrison-Kimmel S., Belokurov V., 2015, MNRAS, 453, 3568
Dooley G. A., Peter A. H. G., Carlin J. L., Frebel A., Bechtol K., Willman B., 2017, MNRAS, 472, 1060
Drlica-Wagner A. et al., 2015, ApJ, 813, 109
Drlica-Wagner A. et al., 2016, ApJ, 833, L5
Erkal D. et al., 2018, MNRAS, 481, 3148
Fattahi A., Navarro J. F., Frenk C. S., Oman K. A., Sawala T., Schaller M., 2018, MNRAS, 476, 3816
Faucher-Giguere C.-A., Lidz A., Zaldarriaga M., Hernquist L., 2009, ApJ, 703, 1416
Ferrero I., Abadi M. G., Navarro J. F., Sales L. V., Gurovich S., 2012, MNRAS, 425, 2817
Fritz T. K., Battaglia G., Pawlowski M. S., Kallivayalil N., van der Marel R., Sohn S. T., Brook C., Besla G., 2018, A&A, 619, A103
Grand R. J. J. et al., 2017, MNRAS, 467, 179
Guo Q. et al., 2011, MNRAS, 413, 101
Helmi A., van Leeuwen F., McMillan P., 2018, A&A, 616, 12
Hunter J. D., 2007, Comput. Sci. Eng., 9, 90
Jethwa P., Erkal D., Belokurov V., 2016, MNRAS, 461, 2212
Kallivayalil N., van der Marel R. P., Alcock C., Axelrod T., Cook K. H., Drake A. J., Geha M., 2006, ApJ, 638, 772
Kallivayalil N. et al., 2018, ApJ, 867, 19
Kim D., Jerjen H., 2015, ApJ, 808, L39
Kim D., Jerjen H., Mackey D., Costa G. S. D., Milone A. P., 2015, ApJ, 804, L44
Koposov S. E., Belokurov V., Torrealba G., Evans N. W., 2015, ApJ, 805, 130
Koposov S. E. et al., 2018, MNRAS, 479, 5343
Laevens B. P. M. et al., 2015, ApJ, 813, 44
Li Y.-S., Helmi A., 2008, MNRAS, 385, 1365
Ludlow A. D., Navarro J. F., Springel V., Jenkins A., Frenk C. S., Helmi A., 2009, ApJ, 692, 931
Luque E. et al., 2016, MNRAS, 458, 603
Lux H., Read J. I., Lake G., 2010, MNRAS, 406, 2312
Lynden-Bell D., 1976, MNRAS, 174, 695
Lynden-Bell D., 1982, The Observatory, 102, 7
McConnachie A. W., 2012, AJ, 144, 4
McKerns M. M., Strand L., Sullivan T., Fang A., Aivazis M. A. G., 2012, preprint (arXiv:eprint)
Marinacci F., Vogelsberger M., 2016, MNRAS, 456, L69
Marinacci F., Pakmor R., Springel V., 2014, MNRAS, 437, 1750
Martin N. F. et al., 2015, ApJ, 804, L5
Moore B., Ghigna S., Governato F., Lake G., Quinn T., Stadel J., Tozzi P., 1999, ApJ, 524, L19
Moster B. P., Somerville R. S., Maulbetsch C., van den Bosch F. C., Macciò A. V., Naab T., Oser L., 2010, ApJ, 710, 903
Nichols M., Colless J., Colless M., Bland-Hawthorn J., 2011, ApJ, 742, 110
Pakmor R., Springel V., Bauer A., Mocz P., Munoz D. J., Ohlmann S. T., Schaal K., Zhu C., 2016, MNRAS, 455, 1134
Pakmor R. et al., 2017, MNRAS, 469, 3185
Pawlowski M. S., 2018, Mod. Phys. Lett. A, 33, 1830004
Perez F., Granger B. E., 2007, Comput. Sci. Eng., 9, 21
Sales L. V., Navarro J. F., Cooper A. P., White S. D. M., Frenk C. S., Helmi A., 2011, MNRAS, 418, 648
Sales L. V., Wang W., White S. D. M., Navarro J. F., 2012, MNRAS, 428, 573
Sales L. V., Navarro J. F., Kallivayalil N., Frenk C. S., 2017, MNRAS, 465, 1879
Sawala T. et al., 2016, MNRAS, 457, 1931
Schaye J. et al., 2015, MNRAS, 446, 521
Shao S., Cautun M., Frenk C. S., Grand R. J. J., Gómez F. A., Marinacci F., Simpson C. M., 2018, MNRAS, 476, 1796
Simon J. D., 2018, ApJ, 863, 89
Simpson C. M., Grand R. J. J., Gómez F. A., Marinacci F., Pakmor R., Springel V., Campbell D. J. R., Frenk C. S., 2017, MNRAS, 478, 548
Springel V., 2010, MNRAS, 401, 791
Springel V., Hernquist L., 2003, MNRAS, 339, 289
Springel V., White S. D. M., Tormen G., Kauffmann G., 2001, MNRAS, 328, 726
Springel V. et al., 2008, MNRAS, 391, 1685
Torrealba G. et al., 2016, MNRAS, 463, 712
Torrealba G. et al., 2018, MNRAS, 475, 5085
van der Marel R. P., Kallivayalil N., 2014, ApJ, 781, 121
van der Walt S., Colbert S. C., Varoquaux G., 2011, Comput. Sci. Eng., 13, 22
Vogelsberger M., Genel S., Sijacki D., Torrey P., Springel V., Hernquist L., 2013, MNRAS, 436, 3031
Wang J., Frenk C. S., Navarro J. F., Gao L., Sawala T., 2012, MNRAS, 424, 2715

This paper has been typeset from a TEX/LATEX file prepared by the author.